




Crystal structure and magnetic properties of $\text{Bi}_{1-x}\text{Ca}_x\text{Fe}_{1-x}\text{Mn}(\text{Ti})_x\text{O}_3$ ceramics across the phase boundary

D. V. Karpinsky^{1,2,*} , I. O. Troyanchuk¹, M. V. Bushinsky², S. A. Gavrilov¹, M. V. Silibin¹, and A. Franz³

¹National Research University of Electronic Technology "MIET", Zelenograd, Moscow, Russia 124498

²Scientific-Practical Materials Research Centre of NAS of Belarus, 220072 Minsk, Belarus

³Helmholtz Zentrum Berlin for Materials and Energy, Berlin, Germany

Received: 24 May 2016

Accepted: 29 July 2016

Published online:

5 August 2016

© Springer Science+Business Media New York 2016

ABSTRACT

Crystal structure and magnetic properties of BiFeO_3 compounds co-doped with Ca and Mn ions as well as Ca and Ti ones were studied using diffraction and magnetometry techniques. Crystal structure of the $\text{Bi}_{1-x}\text{Ca}_x\text{Fe}_{1-x}\text{Mn}_x\text{O}_3$ ceramics with $x < 0.19$ was attested to be single phase rhombohedral one, structural data obtained for the compounds co-doped with Ca and Ti ions testify stability of the polar rhombohedral state up to the concentration level of 25 %. Co-doping with Ca and Mn ions gradually modifies magnetic structure of the compounds toward weak ferromagnetic one; there is no correlation observed between the type of structural distortion and magnetic structure of the compounds. The $\text{Bi}_{1-x}\text{Ca}_x\text{Fe}_{1-x}\text{Mn}_x\text{O}_3$ compounds with $x > 0.25$ show complex magnetic behavior associated with the coexistence of antiferromagnetic matrix and magnetic clusters. Compounds co-doped with Ca and Ti ions with rhombohedral structure testify nearly three times larger remnant magnetization as compared with that observed for Ca | Mn-doped series, and magnetic state of the compounds with $x > 0.1$ remains to be homogeneous weak ferromagnetic one up to $x \sim 0.3$, and above this concentration, magnetic structure is disrupted because of diamagnetic dilution.

Introduction

BiFeO_3 -based materials with perovskite-like structure have attracted great attention of researchers as these compounds possess both magnetic and dipole ordering well above room temperature [1, 2]. To make these materials promising for industrial

applications it is necessary to release remnant magnetization canceled because of modulated magnetic structure [3, 4]. Spatially modulated magnetic structure can be destroyed by strong external magnetic field [5], via thin film preparation [6] or chemical substitution in A and/or B positions of perovskite structure [7–10]. Using chemical substitution, it is

Address correspondence to E-mail: karpinsky@physics.by

possible to modify magnetic subsystem of the compounds and control transport properties and dipole ordering which makes this method to be flexible tool to manage physical properties of the BiFeO₃-based compounds.

Recent studies of the substituted BiFeO₃ materials testify an improvement of the physicochemical properties of the doped compounds with compositions near the phase boundary regions [11–15]. Improved properties of these compounds have been associated with structural instability observed near the phase boundaries, wherein the mentioned metastable state is highly sensitive for external stimuli as electric/magnetic field, temperature, pressure, etc. [8, 16, 17]. Because of the reduced structural stability of the BiFeO₃-based compounds near the phase boundaries, a number of oxygen vacancies, and other structural defects, the estimation of the crystal structure becomes a real technological and scientific challenge. It is assumed that the two-phase structural state usually observed within the phase boundary is characterized by nanoscale size of the coexistent phases, which strongly hampers clarification of their structural symmetry [18, 19]. Determination of the crystal structure and the phase stability regions is also complicated as a variety of available structural data testify different and often contradictive results because of diverse synthesis methods used to prepare the samples [20–23].

To understand the correlation between structural parameters and improvement of the physical properties of the compounds, it is necessary to perform careful study of the crystal structure evolution across the phase boundaries and to trace the related parameters specific for improved physical properties. We have studied BiFeO₃-based solid solutions co-doped with Ca and Ti(Mn) ions with compositions near the phase boundaries which demonstrated enhanced magnetic and ferroelectric properties [11, 24, 25]. Chemical substitution in both perovskite positions permits to extent the phase stability region of the polar rhombohedral phase as well as to estimate the evolution of the magnetic subsystem of the compounds. At present time, a lack of structural data available for these systems prevents an understanding of the improvement of the physical properties as a function of phase stability regions and structural parameters.

In the current study, we have reported the evolution of the phase stability regions and magnetization data for Bi_{1-x}Ca_xFe_{1-x}Ti(Mn)_xO₃ as a function of the dopants concentration and temperature. It should be noted that careful analysis of the magnetic properties is necessary to define the background of remnant magnetization of the compounds having dominant antiferromagnetic structure and to assure the absence of the magnetic impurities. The present study is focused on the magnetic properties of the compounds across the rhombohedral–orthorhombic phase boundary; the magnetic properties of the systems are discussed, assuming different types of the exchange interactions stabilized between transition metal ions depending on structural parameters and electronic configuration of these ions. Understanding the mechanism of the improvement of physical properties of the BiFeO₃-based compounds near the phase boundaries and the factors causing structural stability of the compounds are of fundamental interest and will bring forward practical perspectives of using BiFeO₃-based compounds as functional materials with controlled physical properties.

Experimental

Ceramic samples of Bi_{1-x}Ca_xFe_{1-x}Ti(Mn)_xO₃ system with dopant concentrations $0 \leq x \leq 0.35$ were prepared by two-stage solid-state reaction technique [8, 11]. High-purity oxides taken in stoichiometric ratio were thoroughly mixed using a planetary ball mill (Retsch PM 200). The ceramics were synthesized at 900–1000 °C with intermittent grinding (synthesis temperature was increased with the dopants concentration) followed by a fast cooling down to room temperature. X-ray diffraction measurements were performed with a PANalytical X'Pert MPD PRO and DRON-3 M diffractometers (Cu-K α radiation), and the XRD patterns were recorded in the 2 theta range of 20°–80° with a step of 0.02°. Neutron powder diffraction (NPD) measurements were performed with a high-resolution neutron powder diffractometer (E9 Firepod, $\lambda = 1.7982$ Å, HZB, Germany). The diffraction data were analyzed by the Rietveld method using the FullProf software package [26]. Magnetization measurements were performed using vibrating sample magnetometer (Cryogenic Ltd) in magnetic fields up to 14 T.

Results and discussion

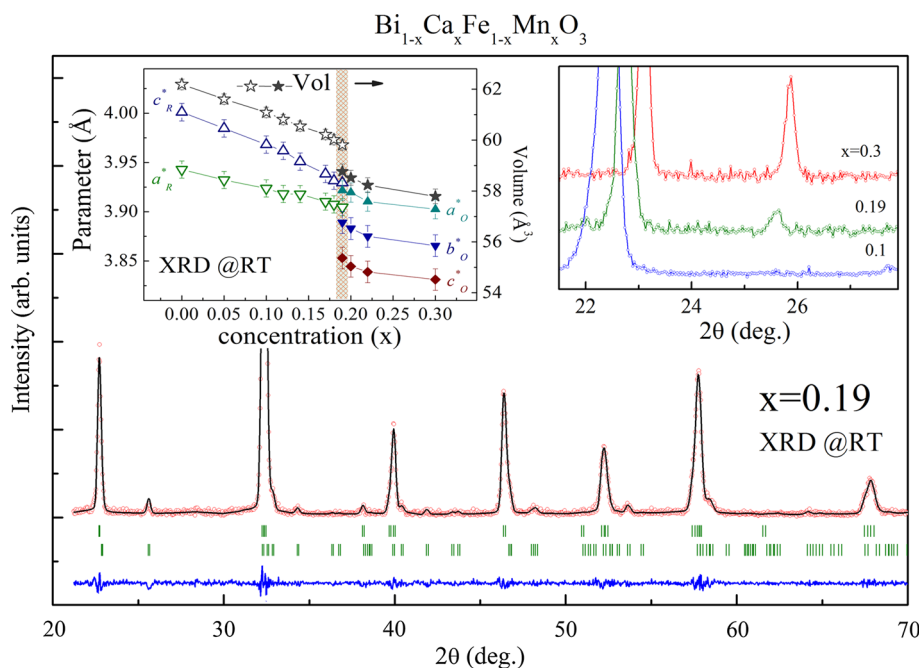
Crystal structure evolution as dopant concentration

Crystal structure of the compounds of both systems has been mainly studied by X-ray diffraction measurements at room temperature. The XRD patterns recorded for the $\text{Bi}_{1-x}\text{Ca}_x\text{Fe}_{1-x}\text{Mn}_x\text{O}_3$ compounds with $x \leq 0.18$ have been successfully refined assuming single phase rhombohedral structure (R3c space group); the compounds with $x \geq 0.2$ have been attested to be single phase with orthorhombic non-polar crystal structure (Fig. 1). The crystal structure of the compound $x = 0.19$ has been described assuming coexistence of the rhombohedral and orthorhombic phases. Narrow concentration region of the two phases (inset, Fig. 1) points to high structural homogeneity of the compounds as compared with other structural data [24, 27, 28]. Diffraction data obtained for the compounds across the phase boundary region did not show any notable broadening of the diffraction reflections (inset, Fig. 1) which also points to high chemical homogeneity of the compounds. Estimated evolution of the crystal structure parameters also testifies a formation of the continuous solid solution with gradual reduction of the unit cell volume and rhombohedral distortion (inset of Fig. 1) followed by prominent decrease in

the unit cell volume (inset, Fig. 1) associated with the structural transition into the orthorhombic phase.

X-ray diffraction data as well as preliminary neutron diffraction measurements performed for some compounds (viz. $x = 0, 0.12, 0.2$) have attested their chemical compositions. It is known that significant difference in the neutron scattering lengths estimated for the constituent ions (viz. for manganese and titanium ions, it is negative while has positive and notably different values for other elements, e.g., for oxygen ions as compared with transition metal ions) has permitted to determine occupation of the ionic positions. Analysis of the diffraction data has confirmed the designed chemical compositions of the samples as well as their oxygen stoichiometry. Assuming electroneutrality of the compositions and electronegativity of the constituent transition metal elements, the most probable electronic configuration of the iron and manganese ions are 3+ and 4+, respectively. The mentioned electronic configurations are in accordance with the available data published for similar systems [29–31] and permit reliable description of the magnetic properties of these compounds as given in the next section. One can conclude certain amount of lattice defects and ionic vacancies due to high temperature synthesis of the samples while their concentration is about negligible amount and does not affect stoichiometry of the compounds. The structural analysis based on the

Figure 1 Refined X-ray diffraction pattern of the compound $\text{Bi}_{0.81}\text{Ca}_{0.19}\text{Fe}_{0.81}\text{Mn}_{0.19}\text{O}_3$ obtained at room temperature. The *line* and *points* refer to the calculated and observed profiles; the *bottom line* represents their difference. Bragg reflections are indicated by *two rows of the tick marks*—*upper* one denotes the rhombohedral phase and *lower ticks* orthorhombic one. The *insets* show the evolution of the unit cell parameters and structural peaks specific for the rhombohedral and/or orthorhombic phases.



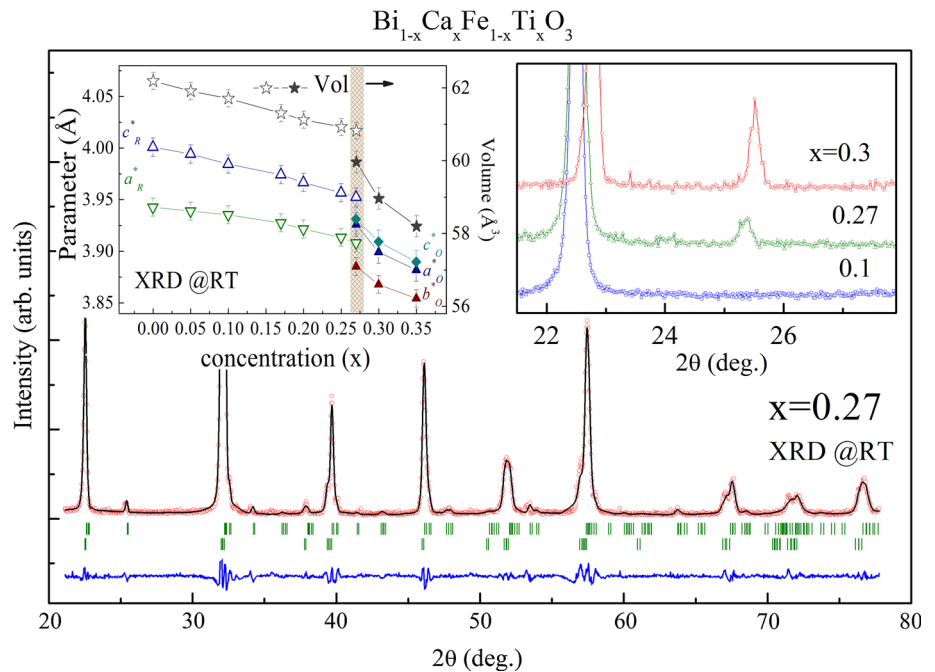
diffraction data has allowed clarify structural parameters which are critical parameters for magnetic properties of the compounds. The refined structural data have revealed an increase of the chemical bond angle Fe|Mn-O-Fe|Mn and corresponding bond length with concentration which is important to estimate the type of exchange interactions between iron and manganese ions.

In contrast to Ca|Mn -doped series, the XRD data recorded for the compounds $\text{Bi}_{1-x}\text{Ca}_x\text{Fe}_{1-x}\text{Ti}_x\text{O}_3$ have testified the polar rhombohedral structural state up to $x = 0.27$ concentration level. Increase in dopant concentration also leads to a reduction of the unit cell parameters and rhombohedral distortion (Fig. 2). It should be noted that the unit cell volume calculated for the $x = 0.27$ compound near the phase boundary is about 2.8 % larger (61.39 vs 59.70 \AA^3) than that observed for similar compound of the Ca|Mn -doped series (inset, Fig. 2), thus indicating that size effect is not the primary aspect causing the phase transition to the orthorhombic structure. Variation in the phase stability range associated with polar rhombohedral structure observed for both systems can be argued by larger ionic radius of the Ti^{4+} ions (compared with Mn^{4+} ones) as well as polar character of the chemical bonds formed by Ti^{4+} ions [32, 33].

The diffraction patterns recorded for the compounds in the concentration range $0.27 \leq x < 0.3$ have been successfully refined assuming coexistence

of the rhombohedral and orthorhombic phases (Fig. 2). Close inspection of the XRD patterns recorded for the compounds in the two-phase region did not reveal any evidence of the intermediate structural phases, whereas certain broadening of the diffraction peaks have been noted for these compounds. A broadening of the diffraction peaks across phase boundary can be directly associated with a minimization of the average size of the structural clusters attributed to the adjacent phases [34, 35]. Quite narrow the two-phase coexistence region confirms high structural homogeneity of the solid solutions which is the result of the optimized synthesis conditions. The crystal structure of the $x \geq 0.3$ solid solutions has been successfully refined assuming centrosymmetric single phase structure with $\sqrt{2a_p} \times \sqrt{2a_p} \times 2a_p$ metric (space group $Pbmm$). It should be noted that temperature increase also leads to structural transformation to nonpolar orthorhombic phase specific for heavily doped compounds. Preliminary temperature dependent diffraction measurements testify gradual reduction in the transition temperature to the orthorhombic phase, e.g., for the compound with Ca|Mn doping concentration of 12 % this transition is completed at $500 \text{ }^\circ\text{C}$ which is significantly lower compared to the transition temperature determined for pristine bismuth ferrite ($\sim 800 \text{ }^\circ\text{C}$) [36]. Further chemical doping results in a reduction of the transition temperature which is valid

Figure 2 Refined X-ray diffraction pattern of the compound $\text{Bi}_{0.73}\text{Ca}_{0.27}\text{Fe}_{0.73}\text{Ti}_{0.27}\text{O}_3$ obtained at room temperature. Two rows of the tick marks denote the orthorhombic (upper row) and the rhombohedral ones (lower ticks). The insets show the evolution of the unit cell parameters and diffraction peaks for the compounds with $x = 0.1, 0.27$, and 0.30 .



for the compounds of both studied systems, thus leading to stabilization of the orthorhombic phase at room temperature as declared for the above-mentioned compositions.

Evolution of the magnetic properties as dopant concentration

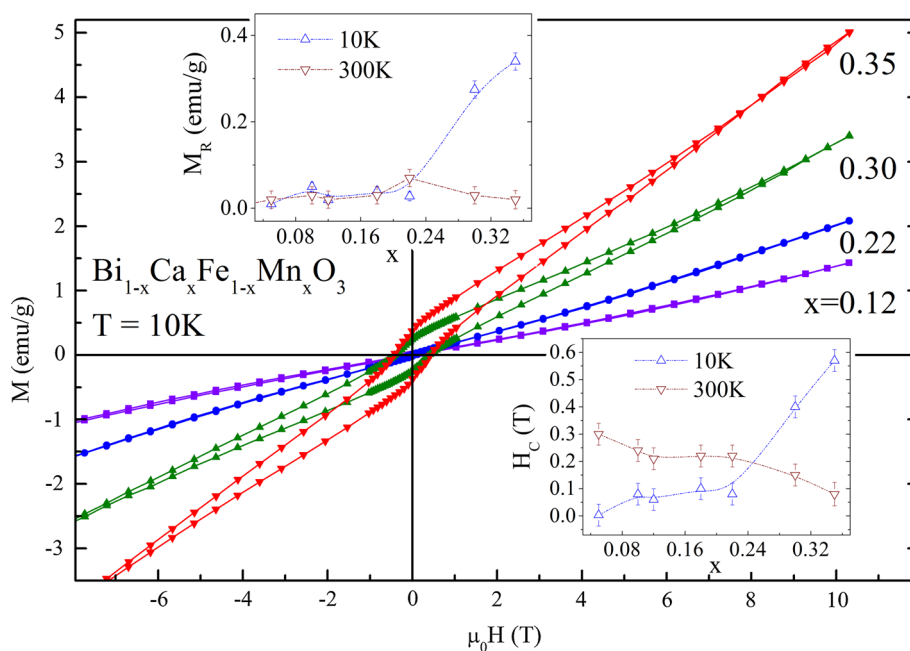
As the compounds of both systems have nearly stoichiometric compositions, the estimated oxygen content is close to the designed 3 ions per primitive unit cell and the manganese and titanium ions are in 4+ oxidation state. Iron ions being in doped compounds in 3+ oxidation state facilitate stabilization of the G-type antiferromagnetic structure in wide concentration range. The magnetic moment calculated based on the NPD data for the moderately doped compound $\text{Bi}_{0.82}\text{Ca}_{0.12}\text{Fe}_{0.88}\text{Mn}_{0.12}\text{O}_3$ is about $2.9 \mu_B$ per formula unit at room temperature. This value is in accordance with the declared electron configuration of the iron ions assuming their occupation level in the perovskite lattice as well as significantly reduced value of magnetization estimated at room temperature. The magnetic moment calculated for this compound at 300°C is about 15 % of that considered at room temperature, thus pointing to reduced temperature of the magnetic transition compared with the transition specific for pristine bismuth ferrite. It should be noted that the model of the magnetic phase used in the refinement process of the NPD data could

not allow distinguish different transition metal ions located in the same crystallographic position of the perovskite structure. The refined data about ionic occupation, the values estimated for the magnetic moments combined with the magnetization data, permitted to determine most reliable electronic configuration of the transition metal ions as well as to estimate the character of magnetic interaction between them.

In spite of the same electronic configuration of the magnetically active iron ions in both systems, the evolution of the magnetic properties is different for these compounds upon temperature and dopant concentration. Most probably, the difference in the magnetic properties is associated with different types of exchange interactions formed between Fe^{3+} and Mn^{4+} and Fe^{3+} and nonmagnetic Ti^{4+} ions; complexity of magnetic state is also caused by uncertainty in the sign of the exchange interaction between Fe^{3+} and Mn^{4+} as it highly dependent on the local structural parameters [37, 38].

Isothermal dependencies of magnetization measured for $\text{Bi}_{1-x}\text{Ca}_x\text{Fe}_{1-x}\text{Mn}_x\text{O}_3$ compounds at $\sim 10\text{ K}$ are depicted in Fig. 3. The $M(H)$ curves of the compounds with doping concentration up to 22 % testify nearly antiferromagnetic behavior; small remnant magnetization ($\sim 0.05\text{ emu/g}$) is caused by a canting of the magnetic moment associated with Dzyaloshinskii-Moriya interactions [39]. Insignificant magnetic hysteresis observed in magnetic fields up to

Figure 3 Field dependencies of magnetization recorded for $\text{Bi}_{1-x}\text{Ca}_x\text{Fe}_{1-x}\text{Mn}_x\text{O}_3$ compounds with $x = 0.12, 0.22, 0.30, \text{ and } 0.35$ obtained at temperature 10 K. The insets show evolution of remnant magnetization and coercive forces of the compounds at temperatures 10 and 300 K.



8–10 T is caused by partial disruption of the spatially modulated spin structure under strong magnetic fields, while this behavior is observed only for the compounds within the rhombohedral crystal structure. It should be noted that structural transformation into the orthorhombic structure does not lead to significant modification of the magnetic structure of the compounds, e.g., isothermal dependence of magnetization obtained for the orthorhombic compound $x = 0.22$ (Fig. 3) testifies behavior similar to that observed for the moderately doped rhombohedral compounds. The magnetization dependencies of the compounds with $x > 0.25$ testify weak ferromagnetic state with remnant magnetization of about 0.25–0.35 emu/g at 10 K which is associated with completely disrupted spatially modulated spin structure (Fig. 3, inset). Increased coercive force observed for these compounds as well as growth of the isothermal magnetization in magnetic fields above 8–10 T testify their inhomogeneous magnetic state at low temperature. It should be noted that temperature increase up to ~ 300 K significantly diminishes magnetization of these compounds as well as their coercivity (Fig. 3, inset), and these results are in accordance with the available data declared for similar compositions [11, 30]. Temperature dependencies of magnetization obtained just after magnetization loop measurements reveals unusual dependences—a decrease of remnant magnetization and coercive force upon temperature drop. This behavior can be explained by a competition between single ions magnetic anisotropy and Dzyaloshinskii–Moriya interaction observed for complex oxides with magnetic sublattices formed by two magnetically active ions similar to the scenario described in Ref. [40].

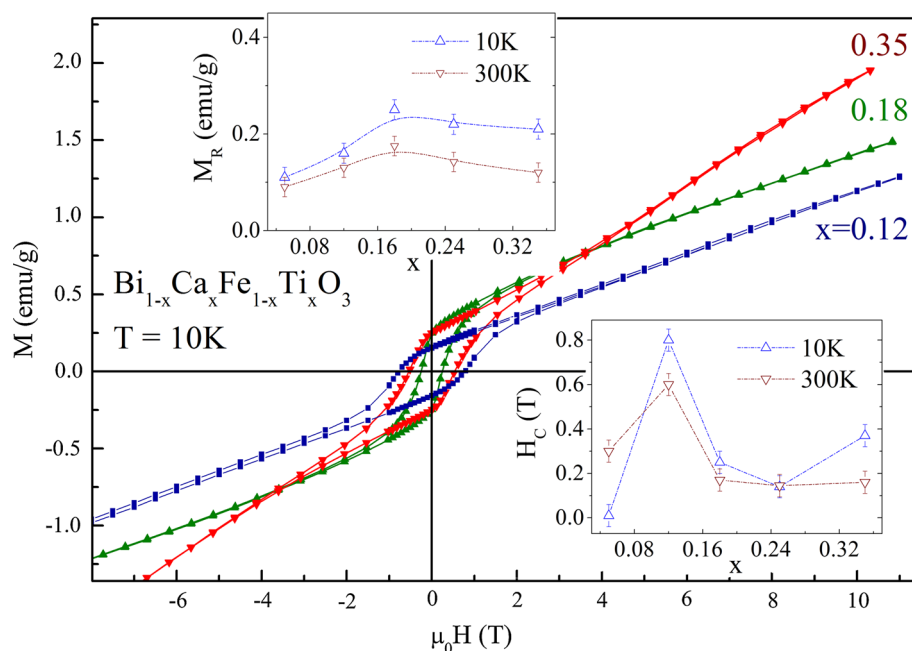
We suppose that the magnetic properties of these compounds are determined by the coexistence of small clusters with dominant ferromagnetic interactions within long-range antiferromagnetic matrix. It is assumed that ferromagnetic-like clusters are stabilized within Mn-rich regions where ferromagnetic behavior can be described assuming superexchange interactions between Fe^{3+} and Mn^{4+} ions which can be reinforced by strong magnetic field. Antiferromagnetic matrix is formed by negative sign interactions between isovalent ions Fe^{3+} – Fe^{3+} and Mn^{4+} – Mn^{4+} ; an increase of manganese ions with weaker exchange interactions (as compared to those between Fe^{3+} ions) leads to a significant reduction of the Neel

point. Suppression of the magnetic transition temperature is approved by nearly linear character of the isothermal magnetization dependencies observed for heavily doped compounds at room temperature (did not shown), and reduction of the remnant magnetization measured at room temperature is shown in Fig. 3 (inset). The mentioned tendency is in accordance with the previously published data for this and similar solid solutions [24, 25].

The isothermal dependencies of magnetization for $\text{Bi}_{1-x}\text{Ca}_x\text{Fe}_{1-x}\text{Ti}_x\text{O}_3$ compounds are depicted in Fig. 4. Increase of the dopant concentration up to $x = 0.12$ leads to a growth of remnant magnetization (~ 0.15 emu/g) and coercive force (~ 0.8 T) which can be caused by inhomogeneous magnetic state (Fig. 4, insets). Most probably magnetic properties of the compound are determined by two magnetic states—one is specific to weak ferromagnetic and the other is characterized by spatially modulated spin structure. Further chemical substitution leads to gradual growth of the remnant magnetization and reduction of the coercivity; the magnetization data obtained for the compound with $x = 0.18$ can be described assuming homogeneous weak ferromagnetic state (coercive force is about 0.2 T) with remnant magnetization of ~ 0.25 emu/g at temperature ~ 10 K. It should be noted that in Ca|Ti-doped system homogeneous magnetic state is stabilized within the rhombohedral structural phase, while pure weak ferromagnetic state of the $\text{Bi}_{1-x}\text{Ca}_x\text{Fe}_{1-x}\text{Mn}_x\text{O}_3$ compounds have been observed only within the orthorhombic phase.

Room-temperature magnetic measurements testify gradual degradation of the magnetically homogeneous state with further chemical substitution (Fig. 4, inset) caused by diamagnetic dilution with Ti ions. The $M(H)$ dependence recorded at 10 K for the $\text{Bi}_{0.65}\text{Ca}_{0.35}\text{Fe}_{0.65}\text{Ti}_{0.35}\text{O}_3$ compound with nonpolar orthorhombic structure testifies increased coercive force up to 0.4 T and reduced remnant magnetization of 0.21 emu/g (Fig. 4, insets). Diamagnetic dilution of the magnetic subsystem of the compounds via doping with Ti ions provides a formation of the inhomogeneous magnetic state where dominant antiferromagnetic matrix coexists with nonmagnetic Ti-rich clusters. It should be noted that magnetic transition temperatures observed for heavily doped compounds $\text{Bi}_{1-x}\text{Ca}_x\text{Fe}_{1-x}\text{Ti}_x\text{O}_3$ are higher compared with those attributed to Ca|Mn series as the latter compounds have frustrated magnetic interactions

Figure 4 Field dependencies of magnetization obtained for $\text{Bi}_{1-x}\text{Ca}_x\text{Fe}_{1-x}\text{Ti}_x\text{O}_3$ compounds with $x = 0.12, 0.18$ and 0.35 obtained at temperature 10 K. The insets show evolution of remnant magnetization and coercive forces of the compounds at temperatures 10 and 300 K.



caused by inhomogeneous magnetic state estimated by magnetization measurements.

Conclusion

Evolution of crystal structure and magnetic properties of BiFeO_3 compounds co-doped with Ca/Mn and Ca/Ti ions were analyzed across the rhombohedral-orthorhombic phase boundary. Chemical substitution with Ca/Mn ions causes structural transition into the orthorhombic phase at the concentration level of 19 %, whereas the rhombohedral phase remains stable up to 25 % upon Ca/Ti doping. Chemical substitution in both series causes modification of magnetic structure from spatially modulated antiferromagnetic into antiferromagnetic one with weak ferromagnetic component, while we could not observe any correlation between the types of structural distortion and magnetic structure of the compounds. Magnetic properties of the $\text{Bi}_{1-x}\text{Ca}_x\text{Fe}_{1-x}\text{Mn}_x\text{O}_3$ compounds were described assuming their inhomogeneous magnetic state caused by the coexistence of long-range antiferromagnetic order along with the short-range clusters having dominant ferromagnetic interactions. BiFeO_3 compounds co-doped with Ca/Ti ions have testified higher magnetization and Neel point as compared with Ca/Mn-doped series wherein magnetic properties of these compounds were described assuming homogeneous weak ferromagnetic state affected by

diamagnetic dilution effects at concentration level above 30 %.

Acknowledgements

This work was supported by the RSF (Project #15-19-20038).

Compliance with ethical standards

Conflict of Interest The authors declare that they have no conflict of interest.

References

- [1] Kadomtseva AM, Popov YF, Pyatakov AP, Vorob'ev GP, Zvezdin AK, Viehland D (2006) Phase transitions in multiferroic BiFeO_3 crystals, thin-layers, and ceramics: enduring potential for a single phase, room-temperature magnetoelectric 'holy grail'. *Ph Transit* 79:1019–1042
- [2] Catalan G, Scott JF (2009) Physics and applications of bismuth ferrite. *Adv Mater* 21:2463–2485
- [3] Sosnowska I, Schäfer W, Kockelmann W, Andersen KH, Troyanchuk IO (2002) Crystal structure and spiral magnetic ordering of BiFeO_3 doped with manganese. *Appl Phys A* 74:s1040–s1042
- [4] Przeniosło R, Palewicz A, Regulski M, Sosnowska I, Ibberson RM, Knight KS (2006) Does the modulated magnetic structure of BiFeO_3 change at low temperatures? *J Phys* 18:2069–2075

- [5] Sosnowska I, Neumaier TP, Steichele E (1982) Spiral magnetic ordering in bismuth ferrite. *J Phys C* 15: 4835–4846
- [6] Ryu S, Kim J-Y, Shin Y-H, Park B-G, Son JY, Jang HM (2009) Enhanced magnetization and modulated orbital hybridization in epitaxially constrained BiFeO₃ thin films with rhombohedral symmetry. *Chem Mater* 21:5050–5057
- [7] Troyanchuk IO, Karpinsky DV, Bushinsky MV, Kovetskaya MI, Efimova EA, Eremenko VV (2012) Morphotropic phase boundary, weak ferromagnetism, and strong piezoelectric effect in Bi_{1-x}Ca_xFeO_{3-x/2} compounds. *J Exp Theory Phys* 113:1025–1031
- [8] Troyanchuk IO, Tereshko NV, Karpinsky DV, Kholkin AL, Kopcewicz M, Barner K (2011) Enhanced piezoelectric and magnetic properties of Bi_{1-x}Ca_xFe_{1-x/2}Nb_{x/2}O₃ solid solutions. *J Appl Phys* 109:114102–114106
- [9] Agarwal RA, Sanghi S, Ahlawat A, Ahlawat N (2012) Structural transformation and improved dielectric and magnetic properties in Ti-substituted Bi_{0.8}La_{0.2}FeO₃ multiferroics. *J Phys D* 45:165001–165009
- [10] Rusakov DA, Abakumov AM, Yamaura K, Belik AA, Van Tendeloo G, Takayama-Muromachi E (2010) Structural evolution of the BiFeO₃–LaFeO₃ system. *Chem Mater* 23:285–292
- [11] Karpinsky DV, Troyanchuk IO, Vidal JV, Sobolev NA, Kholkin AL (2011) Enhanced ferroelectric, magnetic and magnetoelectric properties of Bi_{1-x}Ca_xFe_{1-x}Ti_xO₃ solid solutions. *Solid State Commun* 151:536–540
- [12] Yoo YJ, Hwang JS, Lee YP et al (2015) Origin of enhanced multiferroic properties in Dy and Co co-doped BiFeO₃ ceramics. *J Magn Magn Mater* 374:669–675
- [13] Yang C-H, Kan D, Takeuchi I, Nagarajan V, Seidel J (2012) Doping BiFeO₃: approaches and enhanced functionality. *Phys Chem Chem Phys* 14:15953–15962
- [14] Karpinsky DV, Troyanchuk IO, Mantytskaja OS et al (2014) Magnetic and piezoelectric properties of the Bi_{1-x}La_xFeO₃ system near the transition from the polar to antipolar phase. *Phys Solid State* 56:701–706
- [15] Karpinsky DV, Troyanchuk IO, Pushkarev NV et al (2015) Evolution of electromechanical properties of Bi_{1-x}Pr_xFeO₃ solid solutions across the rhombohedral–orthorhombic phase boundary: role of covalency. *J Alloys Compd* 638:429
- [16] Kan D, Palova L, Anbusathaiiah V et al (2010) Universal behavior and electric-field-induced structural transition in rare-earth-substituted BiFeO₃. *Adv Funct Mater* 20: 1108–1115
- [17] Karpinsky DV, Troyanchuk IO, Tovar M et al (2014) Temperature and composition-induced structural transitions in Bi_{1-x}La(Pr)_xFeO₃ ceramics. *J Am Ceram Soc* 97:2631–2638
- [18] Seidel J, Trassin M, Zhang Y et al (2014) Electronic properties of isosymmetric phase boundaries in highly strained Ca-doped BiFeO₃. *Adv Mater* 26:4376–4380
- [19] Karpinsky DV, Troyanchuk IO, Tovar M, Sikolenko V, Efimov V, Kholkin AL (2013) Evolution of crystal structure and ferroic properties of La-doped BiFeO₃ ceramics near the rhombohedral-orthorhombic phase boundary. *J Alloys Compd* 555:101–107
- [20] Arnold D (2015) Composition-driven structural phase transitions in rare-earth-doped BiFeO₃ ceramics: a review. *IEEE Trans Ultrason Ferroelectr Freq Control* 62:62–82
- [21] Perejon A, Sanchez-Jimenez PE, Perez-Maqueda LA et al (2014) Single phase, electrically insulating, multiferroic La-substituted BiFeO₃ prepared by mechanosynthesis. *J Mater Chem C* 2:8398–8411
- [22] Du Y, Cheng ZX, Shahbazi M, Collings EW, Dou SX, Wang XL (2010) Enhancement of ferromagnetic and dielectric properties in lanthanum doped BiFeO₃ by hydrothermal synthesis. *J Alloys Compd* 490:637–641
- [23] Khomchenko VA, Kiselev DA, Kopcewicz M et al (2009) Doping strategies for increased performance in BiFeO₃. *J Magn Magn Mater* 321:1692–1698
- [24] Kumar P, Shankhwar N, Srinivasan A, Kar M (2015) Oxygen octahedra distortion induced structural and magnetic phase transitions in Bi_{1-x}Ca_xFe_{1-x}Mn_xO₃ ceramics. *J Appl Phys* 117:194103–194116
- [25] Yin LH, Song WH, Jiao XL et al (2009) Multiferroic and magnetoelectric properties of Bi_{1-x}Ba_xFe_{1-x}Mn_xO₃ system. *J Phys D* 42:205402–205406
- [26] Rodríguez-Carvajal J (1993) Recent advances in magnetic structure determination by neutron powder diffraction. *Physica B* 192:55–69
- [27] Karimi S, Reaney I, Han Y, Pokorny J, Sterianou I (2009) Crystal chemistry and domain structure of rare-earth doped BiFeO₃ ceramics. *J Mater Sci* 44:5102–5112. doi:10.1007/s10853-009-3545-1
- [28] Xu B, Wang D, Íñiguez J, Bellaiche L (2014) Finite-temperature properties of rare-earth-substituted BiFeO₃ multiferroic solid solutions. *Adv Funct Mater* 23:552–558
- [29] Khomchenko VA, Paixão JA (2016) Ti doping-induced magnetic and morphological transformations in Sr- and Ca-substituted BiFeO₃. *J Phys* 28:166004–166009
- [30] Yin LH, Sun YP, Zhang FH et al (2009) Magnetic and electrical properties of Bi_{0.8}Ca_{0.2}Fe_{1-x}Mn_xO₃ (0 ≤ x ≤ 0.5). *J Alloys Compd* 488:254
- [31] Sosnowska IM (2009) Neutron scattering studies of BiFeO₃ multiferroics: a review for microscopists. *J Microsc* 236:109–114
- [32] Kothai V, Senyshyn A, Ranjan R (2013) Competing structural phase transition scenarios in the giant tetragonality

- ferroelectric BiFeO₃–PbTiO₃: isostructural vs multiphase transition. *J Appl Phys* 113:084102–084109
- [33] Karpinsky DV, Troyanchuk IO, Sikolenko V, Efimov V, Kholkin AL (2013) Electromechanical and magnetic properties of BiFeO₃–LaFeO₃–CaTiO₃ ceramics near the rhombohedral–orthorhombic phase boundary. *J Appl Phys* 113:187218–187223
- [34] Schönau KA, Knapp M, Maglione M, Fuess H (2009) In situ investigation of the stability field and relaxation behavior of nanodomain structures in morphotropic Pb[Zr_{1–x}Ti_x]O₃ under variations in electric field and temperature. *Appl Phys Lett* 94:122902–122904
- [35] Schönau KA, Schmitt LA, Knapp M et al (2007) Nanodomain structure of Pb[Zr_{1–x}Ti_x]O₃ at its morphotropic phase boundary: investigations from local to average structure. *Phys Rev B* 75:184117–184126
- [36] Selbach SM, Tybell T, Einarsrud MA, Grande T (2008) The ferroic phase transitions of BiFeO₃. *Adv Mater* 20:3692–3696
- [37] Troyanchuk IO, Karpinsky DV, Lobanovsky LS, Franz A, Silibin MV, Gavrilov SA (2016) Magnetic properties and magnetoresistance in La_{0.5}Sr_{0.5}Co_{1–x}Me_xO₃ (Me = Cr, Ga, Ti, Fe) cobaltites. *Mater Res Express* 3:016101–016107
- [38] Karpinsky DV, Troyanchuk IO, Silibin MV et al (2016) Structure and magnetic interactions in (Sr, Sb)-doped lanthanum manganites. *Phys B* 489:45–50
- [39] Ederer C, Spaldin NA (2005) Weak ferromagnetism and magnetoelectric coupling in bismuth ferrite. *Phys Rev B* 71:060401–060404
- [40] Mao J, Sui Y, Zhang X et al (2011) Temperature- and magnetic-field-induced magnetization reversal in perovskite YFe_{0.5}Cr_{0.5}O₃. *Appl Phys Lett* 98:192510–192511